Repository of the Max Delbrück Center for Molecular Medicine (MDC) in the Helmholtz Association

https://edoc.mdc-berlin.de/18831

Deficiency in $I\kappa B\alpha$ in the intestinal epithelium leads to spontaneous inflammation and mediates apoptosis in the gut

Mikuda N., Schmidt-Ullrich R., Kärgel E., Golusda L., Wolf J., Höpken U.E., Scheidereit C., Kühl A.A., Kolesnichenko M.

This is the final version of the accepted manuscript, which was published first in:

Journal of Pathology 2020 MAR 28 (accepted manuscript first published online) doi: 10.1002/path.5437

Publisher: Wiley

This article is protected by copyright. All rights reserved.

Notice

This manuscript was published open access by Wiley.

The article will be published soon under the Creative Commons Attribution 4.0 International License.

Open Access funding is provided by Projekt DEAL.

Deficiency in $I_{\kappa}B\alpha$ in the intestinal epithelium leads to spontaneous inflammation and mediates apoptosis in the gut

Nadine Mikuda,^{1*} Ruth Schmidt-Ullrich,^{1*} Eva Kärgel,¹ Laura Golusda,² Jana Wolf,³ Uta E. Höpken,⁴ Claus Scheidereit,¹ Anja A. Kühl,² Marina Kolesnichenko¹

¹Signal Transduction in Tumour Cells, Max Delbrück Centre for Molecular Medicine, Robert-Rössle-Strasse 10, 13125 Berlin, Germany; ² Charité-Universitätsmedizin Berlin, corporate member of Freie Universität Berlin, Humboldt-Universität zu Berlin, and Berlin Institute of Health; iPATH.Berlin – Core Unit for Immunopathology ³ Mathematical Modelling of Cellular Processes, Max Delbrück Centre for Molecular Medicine, Berlin, Germany ⁴ Microenvironmental Regulation in Autoimmunity and Cancer, Max Delbrück Centre for Molecular Medicine, Berlin, Germany

These authors contributed equally to this work.

This article has been accepted for publication and undergone full peer review but has not been through the copyediting, typesetting, pagination and proofreading process which may lead to differences between this version and the Version of Record. Please cite this article as doi: 10.1002/path.5437

Raw data: <u>https://www.ncbi.nlm.nih.gov/geo/query/acc.cgi?acc=GSE139251</u> Token: mrmvsiwgdzgzpov

Conflict of Interest: The authors of the manuscript declare that they have no conflict of interest

Correspondence: <u>marina.k@oxfordalumni.org / marina.kolesnichenko@mdc-berlin.de</u> Tel. +49 30 94063738 Robert-Rössle Straße 10, Berlin-Buch 13125, Germany

Running title: Constitutive NF-kB mediates apoptosis in intestinal epithelium

Abstract:

The $I\kappa$ B-Kinase (IKK)-NF- κ B signalling pathway plays a multifaceted role in inflammatory bowel disease (IBD): on the one hand, it protects from apoptosis; on the other, it activates transcription of numerous inflammatory cytokines and chemokines. Although several murine models of IBD rely on disruption of IKK-NF-κB signalling, these involve either knockouts of a single family-member of NF-κB, or of upstream kinases that are known to have additional, NF- κ B-independent, functions. This has made the distinct contribution of NF- κ B to homeostasis in intestinal epithelium cells difficult to assess. To examine the role of constitutive NF-kB activation in intestinal epithelial cells, we generated a mouse model with a tissue-specific knockout of the direct inhibitor of NF-κB, *Nfkbia*/IκBα. We demonstrate that constitutive activation of NF- κ B in intestinal epithelial cells induces several hallmarks of IBD including increased apoptosis, mucosal inflammation in both the small intestine and the colon, crypt hyperplasia, and depletion of Paneth cells, concomitant with aberrant Wnt signalling. To determine which NF- κ B-driven phenotypes are cell-intrinsic, and which are extrinsic and thus require the immune compartment, we established a long-term organoid culture. Constitutive NF-kB promoted stem-cell proliferation, mis-localisation of Paneth cells, and sensitisation of intestinal epithelial cells to apoptosis in a cell-intrinsic manner. Increased number of stem cells was accompanied by a net increase in Wnt activity in organoids. Because aberrant Wnt signalling is associated with increased risk of cancer in IBD patients and because NFKBIA has recently emerged as a risk locus for IBD, our findings have critical implications for the clinic. In a context of constitutive NF- κ B, our findings imply that general anti-inflammatory or

immunosuppressive therapies should be supplemented with direct targeting of NF- κ B within the epithelial compartment in order to attenuate apoptosis, inflammation, and hyperproliferation.

Keywords: Inflammatory bowel disease, animal model, NF-κB, precision medicine, inflammation, intestinal organoids, Wnt, stem cells, crypts

INTRODUCTION:

IBD refers to autoimmune disorders, including ulcerative colitis (UC) and Crohn's disease (CD), which cause relapsing inflammation of the gastrointestinal tract [1,2]. Unlike in UC, where inflammation is mainly restricted to the colon and the rectum, in CD, the whole gastrointestinal tract can be affected, and the majority of patients present with terminal ileitis. Patients with IBD are at an increased risk of developing colorectal cancer later in life [3]. Hallmarks of IBD include an aberrant inflammatory response, increased apoptosis in intestinal epithelial cells (IEC), loss of epithelial barrier function, reduction in protective secretory Paneth cells, and dysbiosis [4-6].

Animal models have been indispensable in studying the pathology of inflammation in IBD [7,8]. The vast majority however focus on disease pathogenesis in the colon, and do not involve the small intestine (SI) [9]. Strikingly, a large fraction of genetically engineered murine models of IBD constitute knock-ins or knockouts in the IKK-NF- κ B signalling pathway. NF- κ B plays a central role in IBD development and progression and the level of activation of NF- κ B correlates with the severity of intestinal inflammation [10].

The transcription factor NF- κ B is composed of five distinct family members that form homoand heterodimers that regulate diverse processes in the cell ranging from proliferation to inflammation, and apoptosis [11]. Stress stimuli, including bacterial toxins, inflammatory cytokines and chemokines, and DNA damage converge on the upstream IKK complex, which

cebt activates NF- κ B by phosphorylating the inhibitor of the transcription factor, I κ B α , and thus targeting it for proteasomal degradation [12]. Liberated NF- κ B activates transcription of numerous target-genes including inflammatory cytokines and chemokines but, importantly, also of *NFKBIA*, the gene coding for I κ B α [11]. Knockout of *Nfkbia*/I κ B α in mice leads to early neonatal lethality, thereby posing an obstacle to studying the effect of activated NF- κ B in the mature gut [13,14]. Consequently, whether I κ B α knockout in the epithelial cells *in vivo*, and concomitant activation of NF- κ B, would lead to inflammation and immune-cell response has remained unclear.

NF-κB directly regulates expression of numerous genes implicated in IBD pathogenesis, yet whether NF-κB plays a pro- or anti-inflammatory role in IECs has long been a matter of debate [10]. On the one hand, activation of NF-κB leads to diverse inflammation-related pathologies [13-16], and direct inhibition of NF-κB family member p65 abrogates established experimental colitis [17]. On the other hand, studies using IEC-specific knockout models that target kinases upstream of NF-κB, specifically IKKγ, IKKβ, and mitogen activated protein kinase kinase kinase 7 (MAP3K7/TAK1), suggest that NF-κB protects cells from apoptosis, thereby maintaining intestinal homeostasis [18-23]. These kinases however regulate additional signalling pathways apart from NF-κB [12]. Indeed we have recently shown that IKK represses activation of numerous inflammatory cytokines and chemokines independently of NF-κB through destabilisation of their mRNA [24]. Because different NF-κB subunits can form functional heterodimers, knockouts of individual family members of NF-κB do not directly address the role of the transcription factor in the pathogenesis of IBD. Therefore a murine model able to differentiate between contributions of IKK versus those of NF- κ B was still missing.

To determine which hallmarks of IBD are attributed to direct activation of NF- κ B and whether the transcription factor plays a pro- or anti-apoptotic role in IEC, we generated mice with a specific I κ B α deletion in intestinal epithelial cells, $I\kappa B\alpha^{IEC-KO}$. We demonstrate that NF- κ B is constitutively activated in the intestinal epithelium of these mice, leading to expression of numerous inflammatory cytokines and chemokines. Surprisingly, despite activated NF- κ B, IEC of I κ B α -deficient mice were not protected from apoptosis and, on the contrary, were more sensitive to cytokine stimulation.

To dissect the cell-intrinsic from -extrinsic phenotypes, we cultured intestinal organoids. We demonstrate that the expression of pro-apoptotic genes and the net increased Wnt activity was a cell-intrinsic phenotype, associated with constitutive NF- κ B. Apoptosis and stem-cell identity in the crypt was mediated by extrinsic factors.

MATERIALS AND METHODS:

Ethical Issues

All aspects of animal care and experimental protocols in this study were approved by the regulatory standards of the Berlin Animal Review Board (LAGeSo Berlin) (Reg. G 0082/13, G0358/13, G0092/18, G0111/19 and X9013/11).

Studies involving animals are reported in accordance with the ARRIVE guidelines [25,26].

Generation of $I\kappa B\alpha^{IEC-KO}$ mice and preparation of murine tissues from in vivo experiments. The generation of mice with floxed *Nfkbia* ($I\kappa B\alpha$ gene) alleles (*B6;129P2-Nfkbia^{tm1Kbp}*) was described previously [27]. $I\kappa B\alpha^{IEC-KO}$ mice were generated by mating *B6;129P2-Nfkbia^{tm1Kbp}* with *Tg(ViI-cre)20Syr* (Villin-Cre) mice [28]. Unless specified, the small intestine of mice between 8-15 weeks of age was used for experiments.

Scoring of inflammation in mice

Scoring was preformed according to previously established guidelines [29].

RNA extraction

Small or large intestine was snap-frozen in liquid nitrogen and homogenized. RNA was extracted using Trizol reagent according to manufacturer's instructions (Thermo Fisher, Waltham, USA).

Western Blot analysis and electrophoretic mobility shift assays (EMSA) These were performed as described previously [24,30].

Artic ente

Immunofluorescence and IHC on paraffin tissue sections

Tissue sections were prepared as described previously [31,32]. For lists of antibodies & reagents, see supplementary material, Supplementary materials. UEA-1 (Sigma-Aldrich, L8146) was prepared according to the manufacturer's instructions and used at 0.2mg/mL final concentration according to the IHC protocol described previously [33].

Antibodies/primer sequences.

These are given in supplementary material, Supplementary materials.

Antibody Array: Proteome profiler (R&D Systems, USA) antibody array was performed on 0.2 mL of serum according to the manufacturer's protocol. Quantification performed with FusionCapt Advanced software.

Quantitative RT-PCR

This was performed using a minimum of two reference genes (*Tbp1, Rpl13a, Hrpt1, Sdha*) according to the manufacturer's protocol (Promega, Madison, USA).

Affymetrix array

Gene expression was measured with mouse Clariom S (Thermo Fisher Scientific, USA) and analyzed using a Transcriptome Analysis Console 4.0. For further details, see supplementary material, Supplementary methods.

Preparation of organoids

Crypts were isolated from 4-5 mice per group as described elsewhere [34]. Organoids were grown for 12 days post extraction. Immunofluorescence on organoids was performed as described elsewhere [35]. For RT-qPCR, 30-40 organoids were lysed in Trizol.

Gene set enrichment analysis (GSEA)

GSEA was performed as described elsewhere [36], using Molecular Signature Database v7.

$I\kappa B\alpha^{IEC-KO}$ mice develop spontaneous intestinal defects and inflammation

To investigate the impact of constitutive NF- κ B signalling on the gut epithelium *in vivo*, we generated $I\kappa B\alpha'^{EC-KO}$ mice lacking functional $I\kappa B\alpha$ in the intestinal epithelium by crossing $I\kappa B\alpha'^{Iox/Ilox}$ mice [27] with *villin*-cre [28] transgenic mice (supplementary material, Figure S1A). Depletion of IkB α in the intestine was confirmed by western blot (Figure 1A and supplementary material, Figure S1B). $I\kappa B\alpha'^{EC-KO}$ mice were born at normal Mendelian ratio, and phenotypically normal. However, from 7 weeks of age $I\kappa B\alpha'^{EC-KO}$ mice but not littermate controls presented with rectal prolapse, and by 42 weeks of age 25% of the $I\kappa Ba'^{EC-KO}$ were affected (Figure 1B). In addition, shorter colon, indicative of inflammation, and increased apoptosis was observed in $I\kappa B\alpha'^{EC-KO}$ mice (Figures 1C-E). To determine if these mice developed spontaneous inflammation and morphological changes associated with colitis, we performed histomorphological scoring as described previously [29]. Even in the absence of additional stimuli (e.g. DSS treatment) low-grade inflammation was detected in the colon (Figure 1F).

In the SI, premature, significantly enlarged Peyer's Patches (PP) were already visible in 4week old animals and became more prominent in adults (Figure 1G-H). Dramatic increase in size was accompanied by increase in the B220 (CD45R) positive B-lymphocyte compartment and the germinal center (Figure 1G and supplementary material, Figure S1C). From eight weeks of age $I\kappa Ba^{IEC-KO}$ mice spontaneously developed mild intestinal inflammation (Figure

11). Increase in infiltration by macrophages (F4/80+) and by T lymphocytes (CD3+) was confirmed by immunohistochemistry and quantified as described previously [29] (Figure 1J and supplementary material, Figure S1D).

Many cytokines that are upregulated in IBD are direct targets of NF- κ B [37]. To determine if inflammation was systemic or confined to the intestine, we performed chemokine/cytokine array on serum of $I\kappa Ba^{IEC-KO}$ – and control littermates (Figure 1K). We detected increased secretion of several mouse homologues of human markers of IBD, including metalloproteinase 3 (MMP3), Platelet Derived Growth Factor (PDGF-BB), Neutrophil gelatinase associated lipocalin (LCN2/Ngal), Macrophage Colony Stimulating factor, (CSF1/mCSF) and CC chemokine ligand 20 (CCL20) (Figure 1K). Because the abovementioned targets are transcriptional targets of NF- κ B (see Gilmore database at <u>www.bu.edu/nf-kb/gene-resources/target-genes/</u>), we next sought to determine whether depletion of IkBα was sufficient to activate NF- κ B and where this activation would take place.

Activated RelA/p65 in epithelium and in the follicle associated epithelium (FAE) of $I\kappa B\alpha^{IEC-KO}$ mice

Whole-body knockout of *Nfkbia*/I κ B α leads to neonatal lethality [13,14]. Nonetheless, increased DNA-binding of NF- κ B is only observed in some tissues and cells of I κ B α KO neonates, such as granulocytes, which suggests that, in most tissues, knockout of *Nfkbia*/I κ B α alone is not sufficient for constitutive NF- κ B activation [14]. To determine if

absence of IkBa in the epithelium of the SI would lead to constitutive activation of NF- κ B, we analysed its DNA-binding activity and phosphorylation. NF- κ B showed robust DNA-binding activity in $I\kappa B\alpha^{IEC-KO}$, but in none of the control littermates (Figure 2A, top panel). To establish whether IKK contributed to activation of NF- κ B, we analysed phosphorylation of p65, a substrate of IKK. Only slight phosphorylation of p65 at S536 was detected. In contrast, in irradiated mouse embryonic fibroblasts (MEFs), strong phosphorylation of S536 was evident, and it was reduced in *Ikbkb* (IKK β) knockout cells, as expected (Figure 2A, lower panel).

To determine where NF-κB was activated in IEC, we visualised translocation of the most prevalent subunit p65 by immunofluorescence. Nuclear translocation of p65 was observed in villous epithelium of the $I\kappa B\alpha^{IEC-KO}$ animals (Figure 2B). Similarly, we detected increased production in the follicle-associated epithelium (FAE) of mutant mice (Figure 2C). To confirm that p65/ NF-κB is activated we analysed expression of its *bona-fide* target genes, *Ccl20, Icam1, Tnf*, and *Tnfaip3* (A20). All four target genes were significantly upregulated (Figure 2D). In summary, we have demonstrated that epithelial knockout of *Nfkbia*/IκBα is sufficient to activate NF-κB/p65 in IEC.

Constitutive NF-κB mediates pro-apoptotic and pro-proliferative signalling in IEC

Since it was previously shown that NF-κB protects against apoptosis, we performed microarray Affymetrix analysis on the SI of 8-11 week old mice to determine whether

deficiency of IkBa and activation of p65 leads to anti-apoptotic gene expression as well as activation of biomarkers associated with IBD. We detected 116 downregulated transcripts, with a fold change of at least 2 between the $I\kappa B\alpha$ -deficient IEC and controls (Figure 3A). Expression of some members of the cytochrome P450 superfamily is significantly reduced in IBD, in part due to NF- κ B activation [38,39]. We detected 12 transcripts belonging to the cytochrome P450 superfamily (CYP3A, CYP2C and CYP2J subfamilies) that showed a dramatic drop in expression in the intestines of the mutant mice (supplementary material, Table S1). Gene Ontology analysis revealed enrichment of downregulated genes in the categories of lipid catabolism, epoxygenases p450 pathway, and drug transport (Figure 3B), with the overarching category of metabolism. Surprisingly, lysozyme (Lyz1) and also other genes that are specific for Paneth cells [40], including mucosal pentraxin (Mptx2), colipase (Clps), and defensin alpha related (Defa-rs), were downregulated in the IkBa-deficient intestines (supplementary material, Table S1). Bulk analysis of the SI by microarray allowed us therefore to identify transcripts that were downregulated in IKBaIEC-KO mice, and also to pinpoint which cells were likely affected.

We also detected 109 transcripts that showed a significant upregulation in IEC (Figure 3A and supplementary material, Table S1). Importantly, both key biomarkers of IBD, *Lcn2* and *Tnf* appeared as the highest upregulated transcripts in the small intestinal epithelium of $I\kappa B\alpha^{IEC-KO}$ animals. Gene Ontology analysis showed enrichment for "acute-phase response" and "cellular response to tumour necrosis factor", with overarching term inflammation (Figure 3B).

Surprisingly, none of the typical anti-apoptotic targets of NF- κ B, comprising the Bcl2 family members, appeared upregulated. In contrast, genes responsible for positive regulation of cell death and apoptosis, including interferon-induced protein with tetratricopeptide repeats 2 (Ifit2), NADPH oxidase (Noxa), and NADPH oxidase 1 (Nox1) were enriched (Figure 3C and supplementary material, Table S1). These data suggest that activation of NF- κ B resulting from deletion of Nfkbia/IkBa triggers a pro-apoptotic program in IEC, and leads to upregulation of IBD associated genes including Lcn2, Tnf, Duox2, and Nos2. GSEA revealed that in addition to NF- κ B, additional signalling pathways were activated (Figure 3D and supplementary material, Table S2). These included transcription factors, including Myc and E2F that regulate proliferation, and JAK-STAT3 and IFN γ signalling, which are associated with inflammatory response. Of note, pro-proliferative gene expression is distinct from the antiapoptotic. The former implies increased cell duplication, whilst the latter indicates survival. We did not detect anti-apoptotic gene expression in $I\kappa B\alpha^{IEC-KO}$ animals. Finally, analysis for associated diseases revealed the terms "Ulcerative Colitis", "Inflammatory Bowel Disease", and "Crohn Disease", among others (supplementary material, Figure S2A and S2B).

Hyperplasia and Paneth cell loss in crypts

Paneth cells reside at the base of small-intestinal crypts, where they synthesise and secrete abundant quantities of anti-microbial peptides and additionally help sustain integrity of the intestinal epithelium [41,42]. Dysfunction of Paneth cells or loss through necroptosis or apoptosis contributes to the pathogenesis of IBD [43,44]. Since genes specific for Paneth

cells were strongly downregulated in the SI of *I*kBa^{IEC-KO} mice, we asked whether the cellular composition of crypts was altered. Microscopic examination revealed hyperplasia in crypts and in the FAE (Figure 4A-C and supplementary material, Figure S3A). Paneth cells were depleted at crypt bases of the mutant animals (Figure 4D-E and supplementary material, Figures S3B-D). Some Paneth cells were mislocalized (Figure 4D, grey arrows), and crypt bases were instead occupied by Ki67+ cells. However, no change in the number of Goblet cells, another secretory cell type, was observed in the SI (supplementary material, Figure S3E). Depletion of Paneth cells was further validated through loss of UEA-1+ (Ulex *europeaeus* agglutinin 1) that stains secretory granules (Figure 4F and supplementary material, Figure S3B lower panels) and by staining for Sox9, which is also present in enteroendocrine cells, but at crypt bases is only in Paneth cells (supplementary material, Figure S3C). Paneth cells support stem-cell function by supplying essential factors [41]. Additionally, T helper cells were recently shown to mediate stem-cell differentiation [45-47]. A significantly lower number of Krt15+ stem cells per crypt were detected in IkBa^{IEC-KO} mice (Figure 4G-H). Krt15 is a marker for long-lived multipotent stem cells, whose expression is increased in Lgr5+ cells [48]. We confirmed reduced expression of Lgr5 by RT-qPCR (Figure -I). A recent single-cell survey of intestinal epithelium identified Lgr5+ and Endothelin 1 (Edn1) as stem-cell specific markers for the least differentiated stem cells (intestinal stem cells (ISC)-I), and Olfactomedin 4 (Olfm4) as a pan-stem cell marker [45]. We detected a significant drop in expression of Edn1, but no significant change in Olfm4 expression (supplementary material, Table S1, Table S2, Figure S3F and Figure S3G). On the contrary,

Olfm4+/Ki67+ stem cells extended into crypt bases (Figures 4J and K). Both *Lgr5* and *Edn1* are targets of Wnt signalling [49,50]. Decrease in mRNA expression of certain Wnt targets detected by bulk analyses can however be indicative of loss of cell types expressing these and not of an overall effect of constitutive NF-κB activation.

Constitutive NF-kB results in aberrant Wnt activity in IEC

To determine which phenotypes resulting from constitutive NF-κB are intrinsic versus extrinsic to IEC, we cultured small intestinal organoids. A significant proportion of organoids derived from IkBa^{IEC-KO} mice were either cystic or spheroid with enlarged crypts (Figure 5A-C and supplementary material, Figure S4A). This morphology is typically expected in a setting where Wnt signalling is activated [51], although a recent study showed that prolonged TNFa exposure can also lead to an appearance of spheroid or cystic organoids [52]. Yet, in vivo, we detected aberrant Wnt signalling: whereas some Wnt targets including Myc, Nos2, Frizzled homologue 7 (Fzd7), and Cd44 were mildly upregulated, others, including Lgr5 and Edn1 dropped in expression (Figure 4I and supplementary material, Table S3 and Figure S3F). As discussed above, this could be due to loss of cells driving Wnt or to extrinsic factors modulating expression of Wnt targets. There was no increase in nuclear β -catenin (Ctnnb1) in these organoids (Figure 5A), unlike what is seen in APC-depleted cells [53]. Nevertheless, we did detect a significant increase in expression of Wnt target genes, including Axin2, Myc, Lgr5, and Sox9 (Figure 5D-F and supplementary material, Figure S4B). Expression of intestinal alkaline phosphatase, Alpi, a marker of enterocytes, was significantly decreased

(Figure 5G). This indicates that constitutive NF- κ B signalling in organoids leads to an increase in *Lgr5* and *Myc* expressing cells at the expense of *Alpi*-expressing enterocytes.

To determine if Paneth cell loss of IKBaIEC-KO mice was due to extrinsic or intrinsic factors we stained intestinal organoids against Lyz1. In contrast to the *in vivo* setting, where clear loss of Paneth cells was observed in the IκBα-deficient epithelium (Figure 4D-F), the *ex vivo* cultures harboured lysozyme-positive cells, albeit mostly in the lumen (Figure 5H). We then co-stained organoids for cleaved caspase-3 and β -galactosidase. The latter is highly expressed in both secretory cell types (Goblet and Paneth) in the mouse intestine (supplementary material, Figure S3D). β-gal-positive cells localised exclusively to the lumen of IκBα-deficient organoids, whereas in control animals many β -gal-positive cells could be seen in the budding crypts (supplementary material, Figure S4C). Epithelial turnover leads to shedding of cells into the lumen of organoids and, as expected, most cells that stained positive for the early apoptosis marker, cleaved-caspase 3, were detected there (supplementary material, Figure S4C). Nevertheless, we did not detect an overall increase in double-positive (β -gal+ and cleaved caspase-3+ cells) in IkBa-deficient organoids. In summary, we have demonstrated that constitutive NF- κ B results in increased proliferation of stem cells, concomitant with net increase in Wnt signalling, and mislocalisation of Paneth cells. These phenotypes are intrinsic to IEC.

Hypersensitivity and apoptosis in $I_{\kappa}B\alpha$ -deficient IEC after cytokine exposure

As shown above, expression of several pro-apoptotic but not anti-apoptotic genes was significantly elevated in the SI of the $I \kappa B a^{IEC-KO}$ mice (Figure 3B-D and supplementary material, Table S1). Nonetheless, since we did not detect an increase in cells undergoing apoptosis in crypts of $I\kappa B\alpha^{IEC-KO}$ mice (data not shown) or in untreated organoids from these animals (supplementary material, Figure S4C), we asked whether $I\kappa B\alpha$ -deficient epithelial cells are more sensitive to stress. To this end, intestinal organoids from the $I\kappa B\alpha^{IEC-KO}$ mice and littermate-controls were used to specifically examine the role of the pro-apoptotic contribution of NF- κ B in the epithelium. As expected, localization of cleaved caspase-3+ cells was restricted to the lumen in untreated organoids (Figure 6A, left panels). Treatment of intestinal organoids with sub-lethal doses of TNF α and INF γ resulted in a strong apoptotic response in the $I\kappa B\alpha$ -deficient organoids, but not in the controls (Figure 6A). In line with these data, we detected an upregulation of pro-apoptotic markers including Tnf, Bax, and Noxa (Figure 6B) in the $I\kappa B\alpha$ -deficient organoids (supplementary material, Figure S4D). These markers showed further increase in expression following TNF α treatment. In summary, these data show that constitutive NF-κB in IEC upregulates expression of pro-apoptotic and inflammatory genes through a cell-intrinsic mechanism, leading to an increased sensitivity to extrinsically-mediated apoptosis.

DISCUSSION

Whether NF-κB plays a protective, anti-apoptotic role in IEC, or drives inflammation and contributes to cell death remains controversial [10,13-15,18,19,21-23,43,54-56]. Furthermore,

previous studies described knockouts of upstream kinases that could affect other signalling pathways, or of individual subunits, which may lead to compensatory upregulation of other NF- κ B family members [57]. To address these questions, we established mice with IEC-specific knockout of the direct inhibitor of NF- κ B, *Nfkbia*/I κ B α . The mouse model displayed several hallmarks of IBD: inflammatory response, mucosal infiltration by CD3+ T cells and F4/80+ macrophages, serological markers associated with IBD, and expression of pro-inflammatory pro-apoptotic cytokines by IEC.

This mouse model does not encompass all aspects of IBD – ulceration, transmural infiltration, and acute inflammation were not detected. $I\kappa Ba^{IEC-KO}$ mice displayed phenotypic variability in the degree of inflammatory response and associated expression of inflammatory cytokines, and also in age of onset of rectal prolapse. We believe this is due to the dual role that $I\kappa Ba$ plays in regulation of NF- κ B: it both thwarts and terminates the response [14]. Here we have shown that NF- κ B is activated even in the absence of additional stimulus. However, differential exposure to extrinsic stimuli in the environment would unleash a feed-forward loop of NF- κ B. This implies that the phenotype of $I\kappa Ba^{IEC-KO}$ mice would worsen progressively with age, and that $I\kappa Ba^{IEC-KO}$ mice would be especially sensitive to extrinsic stimuli.

Even in the absence of an additional stimulus, NF- κ B was constitutively activated in the I κ B α deficient epithelium, and drove transcription of pro-apoptotic-, but not of anti-apoptotic genes. IECs underwent apoptosis in response to sub-lethal doses of cytokines.

Previous studies examining the contribution of NF-κB to epithelial homeostasis discovered that tissue-specific knockout of upstream activator IKKγ leads to the expression of inflammatory cytokines and also triggers apoptosis [19,58]. The anti-apoptotic role observed in this model may be due to an NF-κB-independent role of IKK. IKKγ inhibits RIP Kinase 1 (RIPK1) and can therefore protect IEC from apoptosis [58] in parallel or independently of NFκB. Overexpression of constitutively active *Ikbkb*/IKKβ [23,56] in part phenocopies *IκBa^{IEC-KO}*. The phenotype could be in part due to constitutive loss of IκBα expression observed in cells expressing constitutively active Ikbkb/IKKβ [56]. It is possible that the protective role of NF-κB stems from activation via IKKβ, which is not the case in the epithelium of *IκBa^{IEC-KO}* mice. These authors also see hypersensitivity to TNFα in their model, and suggest that persistent activation of NF-κB would upregulate pro-apoptotic functions and shift the balance towards cell death [56]. Our results provide experimental evidence for this hypothesis and reveal that, in the absence of activated IKK, NF-κB alone plays a pro-apoptotic role in IEC.

In line with this, a study showing IEC-specific deletion of an indirect inhibitor of NF- κ B, *Tnfaip3*/A20, [15] corroborates the pro-apoptotic role of NF- κ B in IEC. These IECs were hypersensitive to TNF α -induced apoptosis [15]. Unlike I κ B α , which directly sequesters NF- κ B in the cytoplasm, A20 functions at several junctions of the pathway, most notably by targeting upstream TRAF2 as well as IKK and RIP [59]. Deficiency of A20 in both the IEC and the myeloid cells leads to a similar phenotype observed in the present study [54].

In our mouse model, constitutive NF- κ B leads to an increase in transcription of its *bona-fide* targets, including of *Tnfaip3/A20*. Nevertheless, NF- κ B is decoupled from upstream signalling. Indeed, we would argue that persistent IKK-NF- κ B signalling that leads to constitutive depletion of I κ B α would ultimately result in a subset of nuclear NF- κ B that is independent of A20 or IKK and thus lead to a partial overlap in phenotype with the $I\kappa B\alpha^{IEC-KO}$ mice.

In parallel to pro-apoptotic signalling we demonstrated that NF-κB positively regulates proliferative response, in a cell-intrinsic manner. Hyperplastic crypts were observed in mutant animals; however, ISC-I were less abundant.

Intestinal stem cells (ISCs) are the cells of origin for early neoplastic lesions [3,60,61]. The extent to which intrinsic factors, such as cell divisions of non-cancerous ISCs contribute to cancer risk, is a matter of debate [62,63]. Two recent studies have shown that an increase in Lgr5+ cell number increases tumour susceptibility [64,65]. In both cases, an extrinsic factor (high fat diet), contributes to the phenotype [64,65]. An elegant recent study showed that a reduction of Lgr5+ cells accelerates tumorigenesis resulting from reduction in competition between ISC and a faster fixation of *Apc*-deficient cells [66]. Since neutral competition between stem cells protects against accumulation of deleterious mutations, fixation of a single clone that contains oncogenic mutations can lead to tumorigenesis [66]. This is in line with the Goldilocks model that proposes that Wnt in a "just right" amount, rather than its excessive

activation, drives tumour formation [67,68]. Aberrant Wnt signalling is observed *in vivo* in our model, in part due to depletion of Paneth cells and altered composition of ISC. Aberrant Wnt signalling increases the probability of hitting the Goldilocks zone and therefore increases the risk of cancer development in IBD patients with constitutive NF-KB activity in IEC.

Our findings are of great importance to the clinic. *NFKBIA* was identified as a risk locus for CD and a link between single nucleotide polymorphism in the 3' UTR of *NFKBIA* and IBD was discovered in at least some cohorts [69-71]. Notably, IkB α protein is processed at a higher rate in the mucosa of CD patients due to increased proteasomal degradation [72]. Our data imply that, in the subset of patients with reduced levels of IkB α , constitutively active NF- κ B would drive expression of a pro-proliferative and pro-apoptotic program in IEC. In addition, NF- κ B would lead to aberrant Wnt expression in crypts, increasing cancer risk for IBD patients. Consequently, constitutive NF- κ B activation in IEC is detrimental and therefore direct targeting of NF- κ B in IEC combined with anti-inflammatory approaches is likely to be more effective.

ACKNOWLEDGEMENTS:

We are very grateful to Gabriele Born (Research Group "Genetics and Genomics of Cardiovascular Diseases" AG Hübner, MDC) for Affymetrix chip hybridization and to Wolf-Hagen Schunck (MDC) for stimulating discussions. We would also like to thank Inge Krahn, Sabine Jungmann, Alexandra Schulze, Sarina Hilke and Janine Wolff for excellent technical

assistance, Sandra Cristina Carneiro Raimundo (Microscopy facility, MDC), and Olga Kolesnichenko for help. Big thank you to Daniela Keyner for keeping everything running smoothly.

AUTHOR CONTRIBUTION:

MK designed the study. MK, NM, RSU, CS, AAK, UEH and JW conceived the study. MK, NM, EK and LG carried out experiments. AAK, EK and MK performed formal data analysis. MK wrote the manuscript. MK, RSU, NM, EK, AAK, UEH and LG edited the manuscript. CS, AAK and UEH acquired funding.

FUNDING:

This work was supported in part by Deutsche Forschungsgemeinschaft DFG SCHE277/8-1, BMBF, CancerSys (ProSiTu) to CS, Deutsche Forschungsgemeinschaft (DFG) SFB1340 to LG and AAK and TRR241 to AAK, and the Helmholtz-Gemeinschaft, Zukunftsthema "Immunology and Inflammation" ZT-0027 to UEH.

REFERENCES:

- 1. Torres J, Mehandru S, Colombel JF, et al. Crohn's disease. Lancet 2017; **389**: 1741-1755.
- 2. Thorsteinsdottir S, Gudjonsson T, Nielsen OH, et al. Pathogenesis and biomarkers of carcinogenesis in ulcerative colitis. *Nat Rev Gastroenterol Hepatol* 2011; **8**: 395-404.
- 3. Spit M, Koo BK, Maurice MM. Tales from the crypt: intestinal niche signals in tissue renewal, plasticity and cancer. *Open Biol* 2018; **8**: 180120.
- 4. Martini E, Krug SM, Siegmund B, et al. Mend Your Fences: The Epithelial Barrier and its Relationship With Mucosal Immunity in Inflammatory Bowel Disease. *Cell Mol Gastroenterol Hepatol* 2017; **4**: 33-46.
- 5. Xavier RJ, Podolsky DK. Unravelling the pathogenesis of inflammatory bowel disease. *Nature* 2007; **448**: 427-434.
- 6. Nunes T, Bernardazzi C, de Souza HS. Cell death and inflammatory bowel diseases: apoptosis, necrosis, and autophagy in the intestinal epithelium. *BioMed Res Int* 2014; **2014**: 218493.
- 7. Mizoguchi A, Takeuchi T, Himuro H, *et al.* Genetically engineered mouse models for studying inflammatory bowel disease. *J Pathol* 2016; **238**: 205-219.
- 8. Wirtz S, Popp V, Kindermann M, *et al.* Chemically induced mouse models of acute and chronic intestinal inflammation. *Nat Protoc* 2017; **12**: 1295-1309.
- 9. Pizarro TT, Arseneau KO, Bamias G, *et al.* Mouse models for the study of Crohn's disease. *Trends Mol Med* 2003; **9**: 218-222.
- 10. Atreya I, Atreya R, Neurath MF. NF-kappaB in inflammatory bowel disease. *J Intern Med* 2008; **263**: 591-596.
- 11. Zhang Q, Lenardo MJ, Baltimore D. 30 Years of NF-kappaB: A Blossoming of Relevance to Human Pathobiology. *Cell* 2017; **168**: 37-57.
- 12. Hinz M, Scheidereit C. The IkappaB kinase complex in NF-kappaB regulation and beyond. *EMBO Rep* 2014; **15**: 46-61.
- 13. Klement JF, Rice NR, Car BD, et al. IkappaBalpha deficiency results in a sustained NF-kappaB response and severe widespread dermatitis in mice. *Mol Cell Biol* 1996; **16**: 2341-2349.
- 14. Beg AA, Sha WC, Bronson RT, *et al.* Constitutive NF-kappa B activation, enhanced granulopoiesis, and neonatal lethality in I kappa B alpha-deficient mice. *Genes Dev* 1995; **9**: 2736-2746.
- 15. Vereecke L, Sze M, Mc Guire C, *et al.* Enterocyte-specific A20 deficiency sensitizes to tumor necrosis factor-induced toxicity and experimental colitis. *J Exp Med* 2010; **207**: 1513-1523.
- 16. Kondylis V, Kumari S, Vlantis K, *et al.* The interplay of IKK, NF-kappaB and RIPK1 signaling in the regulation of cell death, tissue homeostasis and inflammation. *Immunol Rev* 2017; **277**: 113-127.

- 17. Neurath MF, Pettersson S, Meyer zum Buschenfelde KH, *et al.* Local administration of antisense phosphorothioate oligonucleotides to the p65 subunit of NF-kappa B abrogates established experimental colitis in mice. *Nat Med* 1996; **2**: 998-1004.
- 18. Kajino-Sakamoto R, Inagaki M, Lippert E, *et al.* Enterocyte-derived TAK1 signaling prevents epithelium apoptosis and the development of ileitis and colitis. *J Immunol* 2008; **181**: 1143-1152.
- 19. Nenci A, Becker C, Wullaert A, *et al.* Epithelial NEMO links innate immunity to chronic intestinal inflammation. *Nature* 2007; **446**: 557-561.
- 20. Greten FR, Eckmann L, Greten TF, *et al.* IKKbeta links inflammation and tumorigenesis in a mouse model of colitis-associated cancer. *Cell* 2004; **118**: 285-296.
- 21. Eckmann L, Nebelsiek T, Fingerle AA, et al. Opposing functions of IKKbeta during acute and chronic intestinal inflammation. *Proc Natl Acad Sci USA* 2008; **105**: 15058-15063.
- 22. Zaph C, Troy AE, Taylor BC, et al. Epithelial-cell-intrinsic IKK-beta expression regulates intestinal immune homeostasis. *Nature* 2007; **446**: 552-556.
- 23. Vlantis K, Wullaert A, Sasaki Y, *et al.* Constitutive IKK2 activation in intestinal epithelial cells induces intestinal tumors in mice. *J Clin Invest* 2011; **121**: 2781-2793.
- 24. Mikuda N, Kolesnichenko M, Beaudette P, *et al.* The IkappaB kinase complex is a regulator of mRNA stability. *EMBO J* 2018; **14**: 24.
- 25. McGrath JC, Drummond GB, McLachlan EM, et al. Guidelines for reporting experiments involving animals: the ARRIVE guidelines. Br J Pharmacol 2010; **160**: 1573-1576.
- 26. Kilkenny C, Browne WJ, Cuthill IC, *et al.* Improving bioscience research reporting: the ARRIVE guidelines for reporting animal research. *PLoS Biol* 2010; **8**: e1000412.
- 27. Rupec RÅ, Jundt F, Rebholz B, *et al.* Stroma-mediated dysregulation of myelopoiesis in mice lacking I kappa B alpha. *Immunity* 2005; **22**: 479-491.
- 28. el Marjou F, Janssen KP, Chang BH, *et al.* Tissue-specific and inducible Cre-mediated recombination in the gut epithelium. *Genesis* 2004; **39**: 186-193.
- 29. Erben U, Loddenkemper C, Doerfel K, *et al.* A guide to histomorphological evaluation of intestinal inflammation in mouse models. *Int J Clin Exp Pathol* 2014; **7**: 4557-4576.
- 30. Kolesnichenko M, Hong L, Liao R, *et al.* Attenuation of TORC1 signaling delays replicative and oncogenic RAS-induced senescence. *Cell Cycle* 2012; **11**: 2391-2401.
- J1. Krieger K, Millar SE, Mikuda N, et al. NF-kappaB Participates in Mouse Hair Cycle Control and Plays Distinct Roles in the Various Pelage Hair Follicle Types. J Invest Dermatol 2018; 138: 256-264.
- Zhang Y, Tomann P, Andl T, et al. Reciprocal requirements for EDA/EDAR/NF-kappaB and Wnt/beta-catenin signaling pathways in hair follicle induction. *Dev Cell* 2009; 17: 49-61.
- 33. Wichner K, Stauss D, Kampfrath B, et al. Dysregulated development of IL-17- and IL-21-expressing follicular helper T cells and increased germinal center formation in the absence of RORγt. FASEB J 2016; **30**: 761-774.

- 34. Sato T, Stange DE, Ferrante M, *et al.* Long-term expansion of epithelial organoids from human colon, adenoma, adenocarcinoma, and Barrett's epithelium. *Gastroenterology* 2011; **141**: 1762-1772.
- 35. O'Rourke KP, Dow LE, Lowe SW. Immunofluorescent Staining of Mouse Intestinal Stem Cells. *Bio Protoc* 2016; **6**: e1732.
- 36. Subramanian A, Tamayo P, Mootha VK, *et al.* Gene set enrichment analysis: a knowledge-based approach for interpreting genome-wide expression profiles. *Proc Natl Acad Sci USA* 2005; **102**: 15545-15550.
- 37. Neurath MF. Cytokines in inflammatory bowel disease. *Nat Rev Immunol* 2014; **14**: 329-342.
- 38. Zordoky BN, El-Kadi AO. Role of NF-kappaB in the regulation of cytochrome P450 enzymes. *Curr Drug Metab* 2009; **10**: 164-178.
- 39. Morgan ET. Impact of infectious and inflammatory disease on cytochrome P450mediated drug metabolism and pharmacokinetics. *Clin Pharmacol Ther* 2009; **85**: 434-438.
- 40. Haber AL, Biton M, Rogel N, *et al.* A single-cell survey of the small intestinal epithelium. *Nature* 2017; **551**: 333-339.
- 41. Clevers HC, Bevins CL. Paneth cells: maestros of the small intestinal crypts. *Annu Rev Physio* 2013; **75**: 289-311.
- 42. Stappenbeck TS. Paneth cell development, differentiation, and function: new molecular cues. *Gastroenterology* 2009; **137**: 30-33.
- 43. Dannappel M, Vlantis K, Kumari S, *et al.* RIPK1 maintains epithelial homeostasis by inhibiting apoptosis and necroptosis. *Nature* 2014; **513**: 90-94.
- 44. Farin HF, Karthaus WR, Kujala P, et al. Paneth cell extrusion and release of antimicrobial products is directly controlled by immune cell-derived IFN-gamma. J Exp Med 2014; **211**: 1393-1405.
- 45. Biton M, Haber AL, Rogel N, *et al.* T Helper Cell Cytokines Modulate Intestinal Stem Cell Renewal and Differentiation. *Cell* 2018; **175**: 1307-1320 e1322.
- 46. Lindemans CA, Calafiore M, Mertelsmann AM, *et al.* Interleukin-22 promotes intestinalstem-cell-mediated epithelial regeneration. *Nature* 2015; **528**: 560-564.
- 47. Naik S, Larsen SB, Cowley CJ, *et al.* Two to Tango: Dialog between Immunity and Stem Cells in Health and Disease. *Cell* 2018; **175**: 908-920.
- -8. Giroux V, Stephan J, Chatterji P, et al. Mouse Intestinal Krt15+ Crypt Cells Are Radio-Resistant and Tumor Initiating. *Stem Cell Reports* 2018; **10**: 1947-1958.
- 49. Barker N, van Es JH, Kuipers J, *et al.* Identification of stem cells in small intestine and colon by marker gene Lgr5. *Nature* 2007; **449**: 1003-1007.
- 50. Kim TH, Xiong H, Zhang Z, *et al.* beta-Catenin activates the growth factor endothelin-1 in colon cancer cells. *Oncogene* 2005; **24**: 597-604.
- 51. Merenda A, Fenderico N, Maurice MM. Wnt Signaling in 3D: Recent Advances in the Applications of Intestinal Organoids. *Trends Cell Biol* 2020; **30**: 60-73.
- 52. Hahn S, Nam MO, Noh JH, *et al.* Organoid-based epithelial to mesenchymal transition (OEMT) model: from an intestinal fibrosis perspective. *Sci Rep* 2017; **7**: 2435.

- 53. Gregorieff A, Clevers H. Wnt signaling in the intestinal epithelium: from endoderm to cancer. *Genes Dev* 2005; **19**: 877-890.
- 54. Vereecke L, Vieira-Silva S, Billiet T, *et al.* A20 controls intestinal homeostasis through cell-specific activities. *Nat Commun* 2014; **5**: 5103.
- 55. Kontoyiannis D, Pasparakis M, Pizarro TT, *et al.* Impaired on/off regulation of TNF biosynthesis in mice lacking TNF AU-rich elements: implications for joint and gut-associated immunopathologies. *Immunity* 1999; **10**: 387-398.
- 56. Guma M, Stepniak D, Shaked H, *et al.* Constitutive intestinal NF-kappaB does not trigger destructive inflammation unless accompanied by MAPK activation. *J Exp Med* 2011; **208**: 1889-1900.
- 57. Steinbrecher KA, Harmel-Laws E, Sitcheran R, *et al.* Loss of epithelial RelA results in deregulated intestinal proliferative/apoptotic homeostasis and susceptibility to inflammation. *J Immunol* 2008; **180**: 2588-2599.
- 58. Vlantis K, Wullaert A, Polykratis A, et al. NEMO Prevents RIP Kinase 1-Mediated Epithelial Cell Death and Chronic Intestinal Inflammation by NF-kappaB-Dependent and -Independent Functions. *Immunity* 2016; **44**: 553-567.
- 59. Shembade N, Harhaj EW. Regulation of NF-kappaB signaling by the A20 deubiquitinase. *Cell Mol Immunol* 2012; **9**: 123-130.
- 60. Fevr T, Robine S, Louvard D, et al. Wnt/beta-catenin is essential for intestinal homeostasis and maintenance of intestinal stem cells. *Mol Cell Biol* 2007; **27**: 7551-7559.
- 61. Barker N, Ridgway RA, van Es JH, *et al.* Crypt stem cells as the cells-of-origin of intestinal cancer. *Nature* 2009; **457**: 608-611.
- 62. Wu S, Powers S, Zhu W, *et al.* Substantial contribution of extrinsic risk factors to cancer development. *Nature* 2016; **529**: 43-47.
- 63. Tomasetti C, Vogelstein B. Cancer etiology. Variation in cancer risk among tissues can be explained by the number of stem cell divisions. *Science* 2015; **347**: 78-81.
- 64. Beyaz S, Mana MD, Roper J, et al. High-fat diet enhances stemness and tumorigenicity of intestinal progenitors. *Nature* 2016; **531**: 53-58.
- 65. Fu T, Coulter S, Yoshihara E, *et al.* FXR Regulates Intestinal Cancer Stem Cell Proliferation. *Cell* 2019; **176**: 1098-1112 e1018.
- 66. Huels DJ, Bruens L, Hodder MC, *et al.* Wnt ligands influence tumour initiation by controlling the number of intestinal stem cells. *Nat Commun* 2018; **9**: 1132.
- 67. Albuquerque C, Breukel C, van der Luijt R, *et al.* The 'just-right' signaling model: APC somatic mutations are selected based on a specific level of activation of the beta-catenin signaling cascade. *Hum Mol Genet* 2002; **11**: 1549-1560.
 - 68. Flanagan DJ, Austin CR, Vincan E, *et al.* Wnt Signalling in Gastrointestinal Epithelial Stem Cells. *Genes* 2018; **9**.
 - 69. Hong SN, Park C, Park SJ, *et al.* Deep resequencing of 131 Crohn's disease associated genes in pooled DNA confirmed three reported variants and identified eight novel variants. *Gut* 2016; **65**: 788-796.

- 70. Szamosi T, Lakatos PL, Szilvasi A, *et al.* The 3'UTR NFKBIA variant is associated with extensive colitis in Hungarian IBD patients. *Dig Dis Sci* 2009; **54**: 351-359.
- 71. Klein W, Tromm A, Folwaczny C, *et al.* A polymorphism of the NFKBIA gene is associated with Crohn's disease patients lacking a predisposing allele of the CARD15 gene. *Int J Colorectal Dis* 2004; **19**: 153-156.
- 72. Visekruna A, Joeris T, Seidel D, *et al.* Proteasome-mediated degradation of IkappaBalpha and processing of p105 in Crohn disease and ulcerative colitis. *The J Clin Invest* 2006; **116**: 3195-3203.
- *73. Piñero J, Queralt-Rosinach N, Bravo A, et al. DisGeNET: a discovery platform for the dynamical exploration of human diseases and their genes. *Database (Oxford)* 2015; **2015**: bav028.

*Cited only in Supplementary material

Figure 1: Abnormal intestinal development and spontaneous mild inflammation in IKBaIEC-KO (A) Whole cell lysates from four IKBaIEC-KO mice and six littermate controls were analysed by SDS-PAGE western blot. Protein expression was analysed with Fusion Solo (Vilber Lourmat) and guantified (Fusion Capt V16.05a). Control was set to 1. Representative blot is shown in Figure S1B. Statistical significance was determined by Mann-Whitney U test. Mean and SD shown. (B) Incidence of rectal prolapse was recorded in *IkBa^{IEC-KO}* and control mice between 1-42 weeks of age. Significance determined by Chi-square test (two-sided) with Yates Correction. (C) Colon length in cm is shown. Two of the five mice with shorter colons also had prolapse. For C-F mice were 32-42 weeks of age. Each point represents data from one animal and median is shown as a black bar. Example for length measurement is shown on the right. Lack of normal distribution in IkBa^{IEC-KO} colons was determined by Shapiro Wilk test and statistical significance was measured by paired Wilcoxon test. (D) Representative images of immunohistochemistry showing cleaved caspase-3+ (red) cells in colon. Scale bars = $20\mu m$. (E) Quantification of cleaved caspase-3+ epithelial cells in the colon. Points represent measurements (10 fields of vision with 100 cells per field) from individual animals in %. Statistical significance was determined by Mann-Whitney U test. Median is shown. (F) Evaluation of histomorphology based on severity of mucosal infiltration, submucosal infiltration and changes of crypt architecture. Scoring system for colon (C) inflammation: Score from 0-12. Median is shown (black bar). Statistical significance was determined by Mann-Whitney U test on $I\kappa Ba^{IEC-KO}$ mice and their littermate controls.

Artic ente

(G) Representative images of immunofluorescence (n=5 per group) stain of PP with DAPI+ nuclei (blue), B220/CD45R+ B cells (green) and CD3+ T cells (red). Scale bars = 50µm. (H) Area per follicle of PP was quantified using ImageJ. PP were quantified in small intestinal sections from IKBa^{IEC-KO} and control mice (>8 weeks of age). Significance calculated by Mann-Whitney U test. (I) Histological inflammation score based on Erben et al. 2014 [29]. Scoring system for small intestinal (SI) inflammation in consequence of cytokine imbalance. Score from 0-5, where 1= mild inflammation (extent: mucosa), 2= mild (mucosa and submucosa), 3= moderate (mucosa and submucosa), 4= marked (mucosa and submucosa and sometimes transmural), 5= marked with submucosal granuloma (mucosa, submucosa, transmural). Statistical significance was determined by paired Student's *t* test; horizontal line represents the median (at 0 in controls). (J) Mean numbers of CD3+ T cells (left) and F4/80+ macrophages (right) within the mucosa of IKBa^{IEC-KO} and control mice. Positive cells were counted in 10 high power fields. Each point indicates average number per animal. Statistical significance was determined by paired Student's t test; horizontal line represents the median (at 0 in controls).

(K) ELISA-based antibody array (R&D Systems Large Mouse Antibody Array) was used to detect serum expression of cytokines in $I\kappa B\alpha^{IEC-KO}$ and control mice (n=4 per group). Cytokines showing significant differences between groups are shown in red for upregulated cytokines and blue for downregulated expression. Significance was determined by Student's *t*-test. Horizontal axis shows fold change.

Figure 2: RelA (p65) is activated in IEC of *IκBa*^{*IEC-K0*} **(A)** Electrophoretic mobility shift assay (EMSA) and SDS-PAGE performed on whole cell lysate (WCL) from bulk small intestine of littermate pairs (n=4 per group). Top panel: EMSA shows DNA binding of NF-κB in littermate pairs. SDS-PAGE western blot on the same lysates from above. As controls, irradiated wt and *Ikbkb* KO (IKKβ) MEFs (10 Gy) were harvested 1h post irradiation. **(B)** Graph shows quantification of nuclear p65 obtained by IF as a ratio (density) between nucleus/cytoplasm analysed using ImageJ (version 2.0.0-rc.69/1.52n). Five mice per group and over 6 sections per mouse were analysed. Whiskers indicate SD; significance was determined by Mann-Whitney *U* test. **(C)** Representative images of IF of the small intestine, including PP. The lines delineate FAE. Scale bars represent 50 µm. Red: p65. Green: Ki67. Blue: DAPI. From n=5 mice per group. Lower panels: higher magnification. **(D)** RNA from bulk small intestine was analyzed by RT-qPCR using primers for the genes shown. Expression was normalized to two reference genes. Significance was determined by Mann-Whitney *U* test. **(C)** Represented the genes shown.

Figure 3: Pro-apoptotic gene signature in $I\kappa Ba^{IEC-KO}$ **mice.** (**A**) RNA extracted from small intestines of mice (n=4 per group) analyzed by Affymetrix microarray. Log2 plot shows the distribution of significantly (P < 0.05) upregulated (red) and downregulated (blue) genes. IkBa is highlighted by a pink circle. (**B**) Transcripts showing significant upregulation or downregulation analysed by DAVID 6.8. Gene Ontology (GO) terms for up- and downregulated transcripts (Significance P < 0.05 Benjamini). GO terms were processed in

Artic ente

REVIGO (semantic similarity setting Jiang&Conarth) to cluster related terms. The plot depicts GO terms associated with upregulated (red) and downregulated (blue) transcripts in $I\kappa B\alpha^{IEC-KO}$ mice (n=4) versus controls (n=4). The X- and Y-axes show semantic space. Circle sizes represent log value prevalence. Proximities of circles to each other depict relationships between GO terms. **(C)** Heatmap showing expression of anti- and pro-apoptotic (DAVID 6.8 apoptosis, *mus musculus*) in mouse pairs (n=4 per group). The key shows expression levels. Genes with at least two-fold change (P < 0.05) between two groups are shown. **(D)** GSEA was performed comparing the $I\kappa Ba^{IEC-KO}$ gene list with the Molecular Signature Database v7. Enrichment plots for top hallmarks are shown. NES = Normalized Enrichment Score; FDR = False Discovery Rate. Hallmarks grouped into two broad categories: proliferation/growth/cell-cycle and inflammatory signalling/apoptosis.

Figure 4: Paneth cell loss accompanies crypt hyperplasia of $I\kappa Ba'^{IEC-KO}$ mice. (A) Representative image of IF of small intestine (n=7 per group) showing Ki67+ proliferating cells (green). Nuclei are stained using DAPI (blue). Red arrows point to crypt bases. Scale bars represent 50 µm. (B) Quantification of crypts showing abundance of Ki67+ cells at crypt bases. Points indicate average % of crypts with the phenotype per animal. Median is shown in clack. Statistical significance was determined by Mann-Whitney *U* test. (C) Average crypt length was measured using ImageJ. Points indicate average (based on 20-30 well-orientated crypts) length per mouse. (D) LYZ1+ Paneth cells (red) at the base of crypts in small intestinal sections in relation to Ki67+ proliferating cells (green); nuclei are stained using DAPI (blue). Scale bars = 50 µm. Grey arrows point to mislocalized Paneth cells. (E) Mean/Median ± SD of

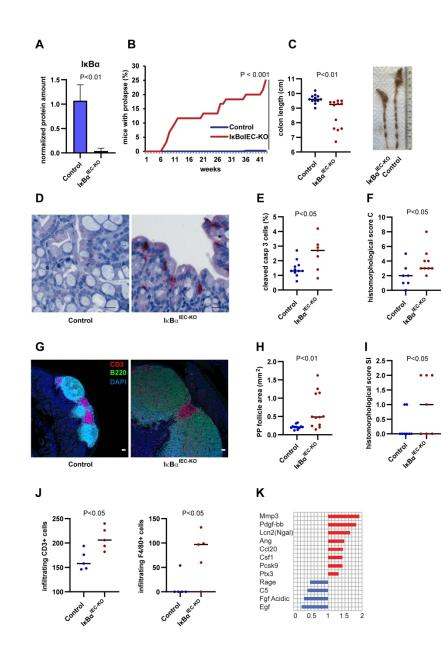
LYZ1+ cells per crypt in >500 crypts per mouse (n=5 per group). Statistical significance was determined by Mann-Whitney test. **(F)** UEA-1 cells at the bottom of 1/3 of crypts (25-30 crypts per mouse, with 5 mice per group) were counted. Statistical significance was determined by Mann-Whitney *U* test. **(G)** Keratin 15 (KRT15)+ stem cells (red) in relation to Ki67+ proliferating cells (green) within the small intestine of $I\kappa Ba^{IEC-KO}$ and control mice (n=6 per group). Nuclei are stained with DAPI (blue). Scale bars = 50 µm. **(H)** Krt15+ cells per crypt in $I\kappa Ba^{IEC-KO}$ and control mice (with 30-40 crypts per mouse, and n=6 mice per group). **(I)** *Lgr5* expression analysed by RT-qPCR from n=6 mice per group. Mean and SD shown. Statistical significance was determined by Mann-Whitney test. **(J)** Pan stem cell marker, Olfm4, positive stem cells (red) in relation to Ki67+ proliferating cells (green), within the small intestine of $I\kappa Ba^{IEC-KO}$ and control mice (n=6 per group). Scale bars = 50µm. **(K)** as in **(J)** but higher magnification, showing double Olfm4+/Ki67+ positive cells in crypt bases.

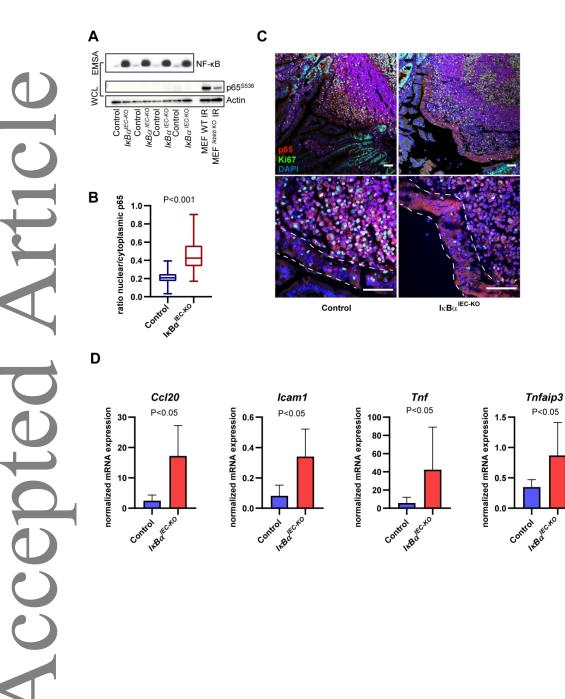
Figure 5: Intrinsic net positive regulation of Wnt by constitutive NF-kB

(A) Small-intestinal organoids stained against active (non-phospho) β -Catenin/Ctnnb1 (red) and E-Cadherin/Cdh1 (green). Scale bars = 50 μ m. Representative images from a total of 20-25 organoids from n=4 mice per group. (B) Percentage of abnormal (cystic or spheroid) organoids was calculated from over 20 organoids per mouse, with n=5 mice per group. Statistical significance was determined by Mann-Whitney *U* test. (C) Crypt diameter was measured in μ m. n=5 mice per group. Statistical significance was determined by Mann-Whitney *U* test. (D) RT-qPCR analysis of *Lgr5* RNA derived from organoids (from n=4 mice per group). Expression was normalized to two reference genes. Statistical significance was determined by Student's *t*-test. Mean and SD shown. (E) As in (D) showing *Axin2* expression. (F) As in (D) showing *Myc* expression. (G) As in (D) showing *Alpi* expression. (H) As in (A) stained with Lyz1 (red) and DAPI (blue). (I) As in (D) ns = not significant.

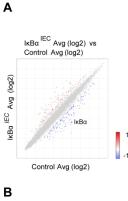
Figure 6: IκBα-deficient IEC undergo cytokine-induced apoptosis. (A) Intestinal organoids from $I\kappa Ba'^{IEC-KO}$ and littermate controls (30-40 organoids from n=3 mice per group) were treated with TNFα or INFγ (10ng/mL) or PBS as an untreated control (UT). After 16 h, organoids were analysed by IF. Representative images from biological replicates (n=5-10 organoids per condition, with n=4 mice per group) show cleaved caspase-3+ apoptotic cells (red) and Ki67+ proliferating cells (green); nuclei are stained with DAPI (blue). Scale bars = 50µm. (B) RNA analysed by RT-qPCR. Expression in control samples was set to 1. Variance was analysed by single way ANOVA. For *Bax*: F = 40.38, *Tnf*. F = 106.88, *Noxa*: F = 194.92. Tukey HSD Post-hoc test for all samples: P value between groups * P < 0.05, ** P < 0.01, *** P < 0.001.

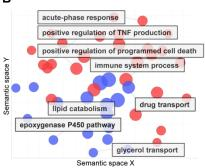
CCCC

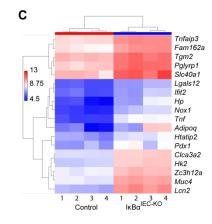












D

Proliferation/growth/cell cycle





NES: 2.55 FDR q-val: <0.001



NES: 2.39 FDR q-val: <0.001





NES: 2.10 FDR q-val: <0.001



NES: 1.91 FDR q-val: <0.001

KRAS_signaling_up

NES: 1.81 FDR q-val: 0.001







INTERFERON_GAMMA_ response



FDR q-val: <0.001



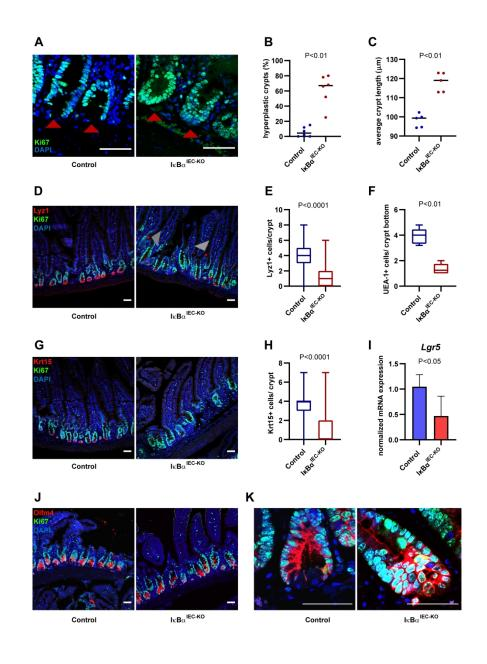




INFLAMMATORY_response



Accept



Accept

D

normalized mRNA expression

Н

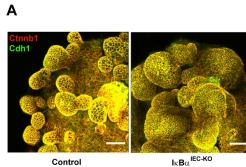
2.0-

1.5

1.0

0.5

0.0



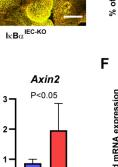
Ε

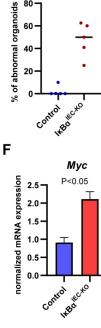
normalized mRNA expression

0

WBG LAND

Control

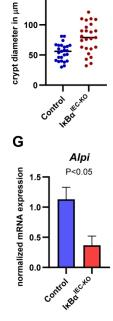




Control

I

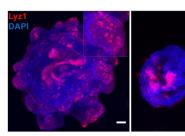
P<0.001



P<0.01

С

150



Lgr5

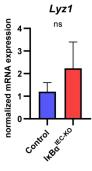
P<0.05

WB0 CHO

Control

Control

IκBα^{IEC-KO}

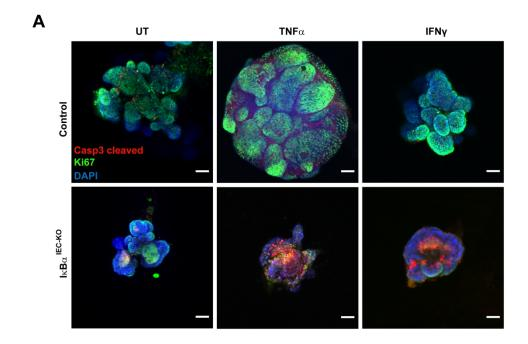


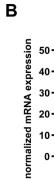
This article is protected by copyright. All rights reserved.

В

80-

60.





0

Accept

